Daniel's Super Cool and overly long title

Daniel Mortensen, Jacob Gunther

***Abstract*—TODO: add abstract**

***Index Terms*—TODO: Add Keywords**

I. Introduction

Recent calls for a reduced carbon footprint have pushed transit authorities to adopt battery electric buses (BEB). Conversion from diesel and CNG to BEB reduces environmental impact as BEB provide zero emissions and access to renewable energy [14].

These benefits are possible because BEB draw power from electrical infrastructure. The loads introduced by charging are substantial and can exceed the grid capacity [16][6][3], requiring prohibitively expensive upgrades. The cost of upgrading is reflected in the billing structure used by power providers and can make large-scale charging undesireable for consumers.

One approach to reducing charge costs is to defer upgrades by efficiently managing when and at what rates buses charge. However, developing charge plans must consider a number of factors. All buses must maintain a minimum charge level while adhering to route schedules. When charging, batteries must have sufficient charge time and share a limited number of chargers. All charging must also be done while other services draw power from the grid, acting as uncontrolled loads. The focus of this work is to find an optimal charge schedule which meets these requirements and minimizes fiscal expenses from grid use in the presence of uncontrolled loads. This problem is refered to hereafter as the 'charge problem'.

The remainder of this paper is organized as follows: Section II gives a description of previous work for solving the charge problem and Section III describes a graph-based framework for modeling the operations environment. Section IV extends the content of III to account for differences between day and night operations, and Section V incorporates the problem constraints involving battery charge dynamics. Sections VI and VII translate the rate schedule used for billing and into an objective function to minimize. Finally, Sections VIII, IX, and X briefly describe the optimization software used to solve the resulting mixed integer linear program developed in previous sections, presents results, and describes future work.

II. Literature Review

We acknowledge the existance of additional contributions, such as minimizing costs for startup infrastructure [17], and preserving battery lifespan [9]. However, as these are not relevent to this work, we consider them outside the scope of this review. We further acknowledge that some works cited herein contain solutions to several of these problems, such as in [20], but for sake of organization, we list them in the most relevent context.

A. Battery Charging

Here we consider solutions to empty batteries and focus our attention on either battery replacement or charging methods. We also refer to charging methods as either static (at rest) or dynamic (in motion).

Because charge times can significantly complicate logistics, [19] and [11] give methods for exchanging spent with charged batteries. The benefits include minimal down time as refueling can occur in a matter of minutes. Unfortunately, batteries can be cumbersome, and their exchange can be difficult. It also requires specialized tools, and could require automation.

Another alternative is to inductively charge buses while they traverse their routes [2], [11], [12], [5]. Unfortunately, this requires significant infrastructure which may not be available and is cost prohibitive for large systems.

Alternative solutions tend towards optimal planning. This allows for buses to charge in the traditional sense, minimizes additional infrastructure, and avoids the complexities of exchanging batteries. These approaches generally fall into one of three categories; reactive, hybrid, and global.

Reactive planning focuses strictly on presential circumstances. Methods of this type are computationally efficient, run in real-time, and are adaptable. These techniques generally stem from control theory and minipulate a current state to minimize cost. One such example includes the work done by [4], who uses comparable methodology to reduce demand on the power grid. This methodology however, does not account for global phenomena that require broader planning schemes and for the most part this class of technqiues remain unused for bus charging.

Another class of algorithms encompasses a limited number of projected events to improve decision making. This allows for a middle ground between simplicity and global planning and has proven useful in previous work [10], [1].

Global planning algorithms assume comlplete foreknowledge of future events and provide globally optimal plans [18],[7]. This class of algorithm requires more computation and is less flexible then reactive or hybrid approaches. However, the solutios are globally optimal and derive from insight unavailable to other algorithm classes.

B. Cost Management

The final set of constraints aim to decrease load on the grid. Previous work has shown that the use of electric buses can significantly complicate local power management [3] [6]. Additinally, power demand generally increases the fiscal cost from a billing perspective. [8] has provided methodology for forcasing the load on the grid. These types of models often form the basis for power distribution algorithms. For example, [15] gives an approach to minimize grid demand, but requires

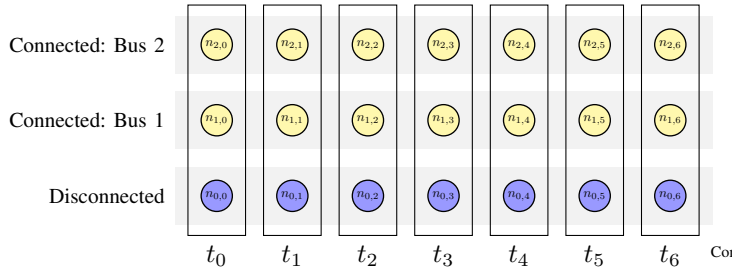

Fig. 1: Graph showing buses and timesteps

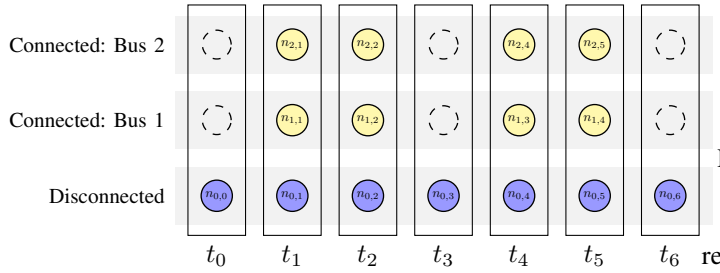

Fig. 2: Bus availability represented in a graph

foreknowledge of uncontrolled loads. [4] takes a different approach and observes real-time data to control the charge rates of connected buses. [13] also operates in the real-time sense but uses on-board batteries to mitigate the effects of rapid charging.

III. Graph Based Problem Formulation

A solution to the bus charge problem must reveal both *when* and *to which* bus a charger should connect suggesting a model with two dimensions. The first dimension characterizes time and is given discretely in a left to right fashion. The second dimension encodes the charger state and extends vertically as seen in figure 1. The charger may occupy one of several states. It may be connected to one of the N buses, or it may be unconnected, giving a total of $N+1$ charge states. The 2-D representation is encoded as a grid where the intersection of charge states and time indices is represented by a node, denoted $n_{i,j}$ which represents the i^{th} charge state at the j^{th} time index (see figure 1).

A complete grid, however, implies that buses are always available to charge. This is not always the case as buses cannot charge when providing transit services. To reflect this constraint, the presence of nodes is used to denote a bus's availability for charging and nodes are removed during times where a bus provides transit services (see figure 2).

Transitions from one node to the next are called edges (see figure 3) and represent decisions to either connect, charge, not charge, or disconnect. The decision an edge represents is determined by the nodes on either end. For example, the edge from $n_{0,0}$ to $n_{0,1}$ in figure 5 represents a period where chargers are idle, resulting in a no-charge decision. This occures because both $n_{0,0}$ and $n_{0,1}$ represent a disconnected charge state. Similarly, the edge between $n_{1,1}$ and $n_{1,2}$ indicates a to-charge decision as both $n_{1,1}$ and $n_{1,2}$ represent states where a bus is connected. Both to-charge and no-charge decisions are

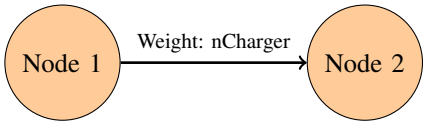

Fig. 3: Node to Node Connection

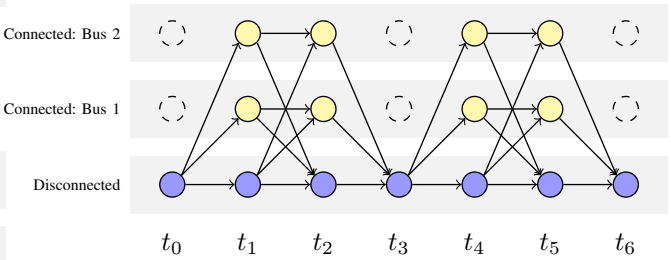

Fig. 4: Graph-based model of the complete decision-space

represented by *horizontal* transitions in the graph and do not change the effective charger state.

Conversely, diagonal transitions represent effective state changes where a charger either connects to or disconnects from a bus. One such example from figure 5 includes the edge from $n_{0,0}$ to $n_{1,1}$. This edge represents an interval where a charger is disconnected at t_j and connected at t_{j+1}, implying a 'to-connect' decision. The same logic applies in reverse for the edge between $n_{1,2}$ and $n_{0,3}$. Hence, the bus charge problem can be described in terms of nodes and edges where nodes represent connectable time instances and edges encode *potential* decisions. Figure 4 shows how the decision space of the two-bus scenario given in figure 2 might be encoded.

Schedule selection is then represented by selecting edges to determine a path through the graph. Edge selection is indicated by the edge weight where the weight value represents the number of chargers in the transition. Therefore, a zero-valued weight represents an unused, or inactive, edge, and an n-valued weight represents an 'active' edge used by n chargers.

Consider a two-charger scenario where buses using the graph in figure 4. A solution where one charger connects to Bus 1 from t_1 to t_2 and Bus 2 from t_4 to t_5 would be

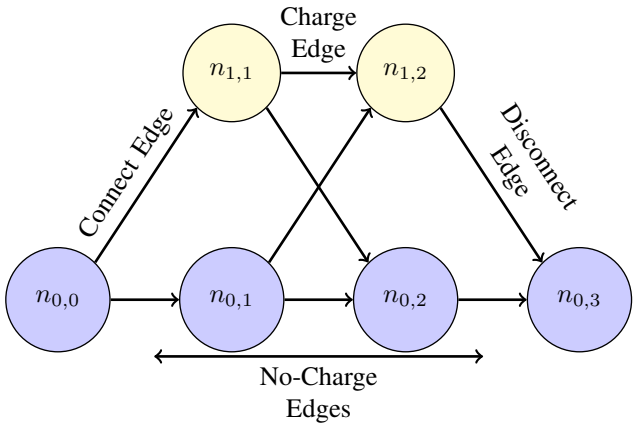

Fig. 5: Connect, Disconnect, and Charge Edges

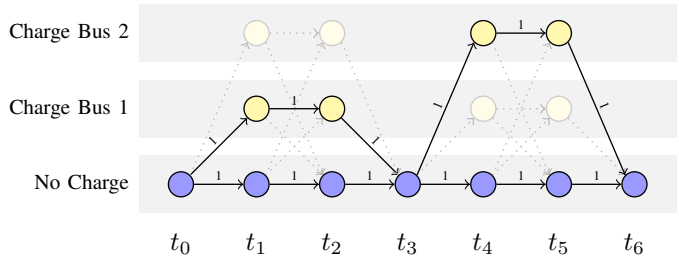

Fig. 6: One solution to a 2-bus 2-charger scenario

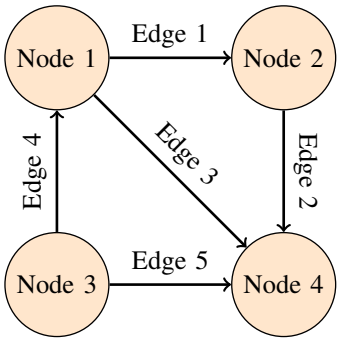

Fig. 7: A generic directed graph consisting of nodes and edges

expressed by assigning non-zero weights to the appropriate connect, charge, and disconnect edges. The second charger remains idle as illustrated by the active edges along the bottom row of charger states (see figure 6). Thus, solving the bus charge problem becomes a matter of finding the optimal set of edge weights.

The bus charge problem aims to minimize the fiscal expense from charging while meeting the operational constraints of a transit system. The graph encodes a subset of these constraints and can be expressed in linear form such that

$$Ax = c_f \tag{1}$$

where A is an incidence matrix, x is an nNode $\times 1$ vector containing edge weights, and c_f is a set of *flow constraints*.

An incidence matrix organizes relationships between nodes and edges by describing which edges depart from and connect to which nodes. An incidence matrix A is an nNode $\times$ nEdge matrix where nNode is the number of nodes, and nEdge is the number of edges. Incoming connections are represented by $A_{i,j} = 1$, where i is the node index, and j corresponds to the edge. Similarly, outgoing connections are given with $A_{i,j} = -1$, and no connection with $A_{i,j} = 0$. For example, the graph in figure 7 is represented as:

$$\begin{bmatrix} -1 & 0 & -1 & 1 & 0 \\ 1 & -1 & 0 & 0 & 0 \\ 0 & 0 & 0 & -1 & -1 \\ 0 & 1 & 1 & 0 & 1 \end{bmatrix} \tag{2}$$

An incidence matrix can be used to find the number of chargers entering and leaving each state. Because the number of chargers must be conserved, the number of incoming and outgoing chargers must be equivalent. This is expressed in linear form as $a_i^T x = 0$, where a_i is the i^{th} row of A. The only exception occurs at *source* and *sink* nodes.

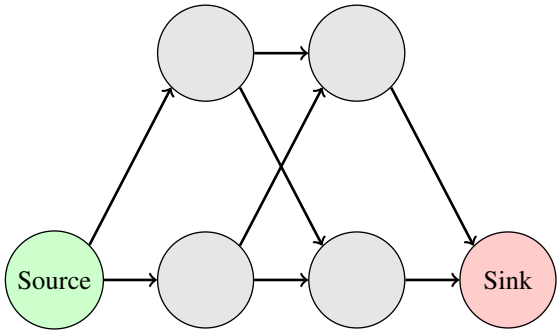

Fig. 8: Network flow illustrating sources and sinks

A source node represents the beginning state for all chargers. Because edge originate here, there are no incoming edges and, the net difference between the representative incoming and outgoing chargers, or *the net-flow*, will be minus the number of chargers. This is described in linear form as $a_i^T x = -\text{nCharger}$.

Sink nodes represent the final state, where all edges terminate (see figure 8). Because sinks have no outgoing edges, they maintain a positive net-flow equal to the number of chargersand are expressed as $a_i^T = \text{nCharger}$.

Therefore, the *flow constraints* represented by c_f are equal to zero at all times except when representing the flow for source and sink nodes as seen in equation 3.

$$Ax = \begin{bmatrix} 0 \\ \vdots \\ -\text{nCharger} \\ \vdots \\ 0 \\ \text{nCharger} \\ \vdots \\ 0 \end{bmatrix} \tag{3}$$

Flow can also be used to ensure that buses connect to only one charger at a time. Let a charge session, or *group*, be the set of all charge nodes between routes as shown in figure 9. The *group flow* is the number of chargers that enter a group and is represented as the sum of all incoming edge weights (see figure 10).

Let B be a nGroup $\times$ nEdge matrix where $B_{i,j}$ is 1 if the j^{th} edge enters the i^{th} group and 0 otherwise. For example, the B matrix corresponding to the graph in figure 11 contains 1 in the 7^{th} and 10^{th} columns for Group 1, and the 12^{th} and 15^{th} columns for group 2 as given in equation 4.

$$B = \begin{bmatrix} 0\,0\,0\,0\,0\,0\,1\,0\,0\,1\,0\,0\,0\,0\,0 \\ 0\,0\,0\,0\,0\,0\,0\,0\,0\,0\,1\,0\,0\,1\,0 \end{bmatrix} \tag{4}$$

Let x be the edge weights as before and c_g be an nGroup $\times$ 1 vector where the i^{th} element gives the group flow for group i. The group flow is then computed as

$$Bx = c_g \tag{5}$$

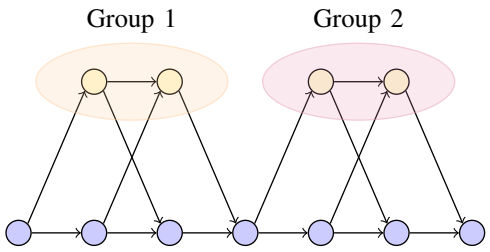

Fig. 9: Example of groups in a network flow graph

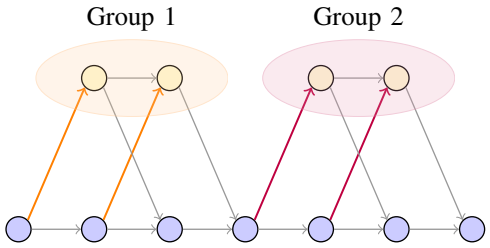

Fig. 10: Incoming Group Edges

But the group flow is required to be one at most. This is expressed by the inequality given in equation 6.

$$Bx \leq \begin{bmatrix} 1 \\ 1 \\ \vdots \\ 1 \end{bmatrix}, \tag{6}$$

IV. Battery State of Charge

Battery state of charge (SOC) also plays a large role in the bus charge problem. As a bus traverses a route, energy is discharged from the battery. If the battery state of charge drops to zero, the bus will power down and become unresponsive. It is therefore important to track battery charge levels when scheduling charge times.

Furthermore, as no charge actions are available while on route, SOC values are only tracked when in the charge station. Because these in-station time periods are also represented by the charge nodes from figure **??**, the two are in one-one correspondence. Consequently, every charge node$_{i,k}$ can be associated with an SOC value, denoted $d_{i,k}$ as shown in figure 12.

Charge level progression between $d_{i,k}$ and $d_{i,k+1}$ is influenced by two factors: discharging on route, and charging. The

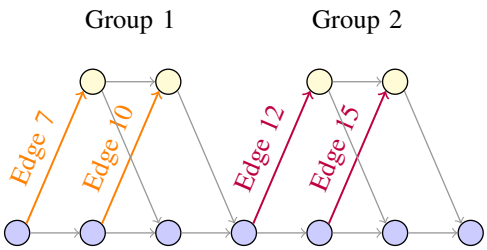

Fig. 11: Connect edge example for groups

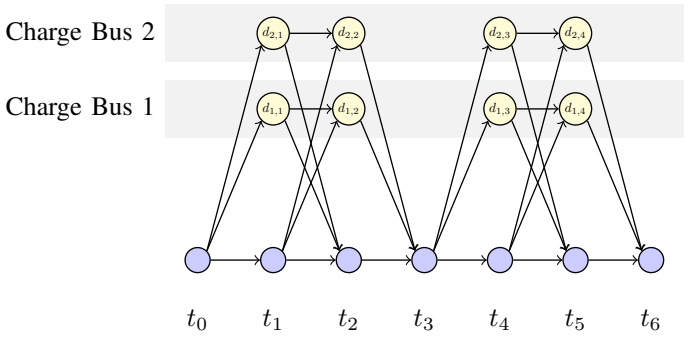

Fig. 12: SOC indicators

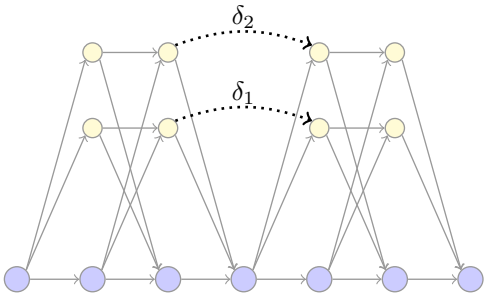

Fig. 13: δ values for routes

route discharge, denoted δ, represents the energy drawn from the battery in kWh. When a bus returns from a route, the change in SOC is computed as

$$d_{i,k+1} = d_{i,k} - \delta_i \tag{7}$$

where δ_i is the discharge for Bus i's route as seen in figure 13.

When a charger connects to a bus, the increase or *gain* in $d_{i,k}$ is denoted $g_{i,k}$, where i and k represent the respective bus and outgoing node indices. Figure 14 gives an example where $g_{1,1}$ and $g_{1,3}$ correspond to Bus 1's gain from t_0 to t_1 and t_4 to t_5.

Using a single charge rate however has drawbacks. If the rate is high, buses will charge quickly but the load on the grid will increase. Decreased charge rates will stress the grid less but increase charge time. To address both situations, a method

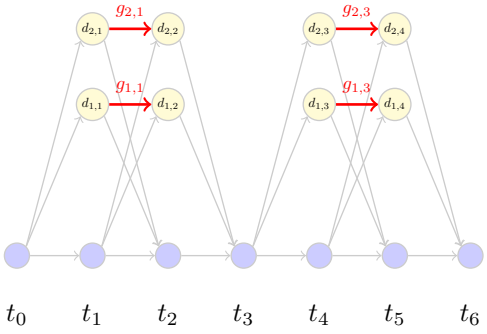

Fig. 14: Depiction of which edges increase SOC for the single rate case

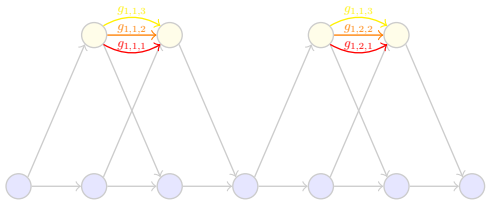

Fig. 15: Multi-Rate Charging

with additional flexibility must be used where both high and low charge rates are available.

Let $g_{i,k,l}$ be the gain, where i and k represent the bus and outgoing node indicies as before and l represents the charge rate index. Each charge rate index corresponds to an edge in the graph. Figure 15 gives an example where there are three rate options. Each rate corresponds to an edge between two charge nodes and together, all three edges provide multiple options for charging. These gains are used to compute succeeding charge levels as

$$d_{i,k+1} = d_{i,k} + \sum_{l} g_{i,k,l}, \tag{8}$$

but because of group and flow constraints, only one charge rate can be active at a time. Therefore, $d_{i,k}$ can be expressed as

$$d_{i,k+1} = d_{i,k} + g_{i,k,l}, \tag{9}$$

where the l^{th} charge edge is active.

$g_{i,k,l}$ is computed using the Constant Current Constant Voltage (CCCV) model as derived in [18] which gives:

$$d_{i,k+1} = \bar{a}_l d_{i,k} - \bar{b}_l M \tag{10}$$

Where $\bar{a}_l \sim (0, 1]$, depends on the charge rate and is experimentally determined, M is the battery charge capacity in kWh, and $\bar{b}_l = \bar{a}_l - 1$. Equations 9 and 10 are used to show that

$$\begin{aligned} & d_{i,k+1} = \bar{a}_l d_{i,k} - \bar{b}_l M \\ \Rightarrow & d_{i,k+1} - d_{i,k} = \bar{a}_l d_{i,k} - \bar{b}_l M - d_{i,k} \\ \Rightarrow & g_{i,k,l} = \bar{a}_l d_{i,k} - \bar{b}_l M - d_{i,k} \\ \Rightarrow & g_{i,k,l} = (\bar{a}_l - 1) d_{i,k} - \bar{b}_l M \end{aligned} \tag{11}$$

The results from equation 11, however, only hold when a charger is connected to a bus, which is represented by a weight of 1 for the edge corresponding to $g_{i,k,l}$. When the weight equals 0, $g_{i,k,l}$ must also equal zero. These two situations can be described using a switching constraint known as the *big M* technique. This technique is used to describe $g_{i,k,l}$ with equation 11 when the transition weight is 1 and $g_{i,k,l} = 0$ when 0.

$$\begin{aligned} & \begin{cases} g_{i,k,l} = d_{i,k}(\bar{a}_l - 1) - \bar{b}_l M & x_{i,k,l} = 1 \\ g_{i,k,l} = 0 & x_{i,k,l} = 0 \end{cases} \\ \Rightarrow & \begin{cases} g_{i,k,l} \le d_{i,k}(\bar{a}_l - 1) - \bar{b}_l M \\ g_{i,k,l} \ge d_{i,k}(\bar{a}_l - 1) - \bar{b}_l M & x_{i,k,l} = 1 \\ g_{i,k,l} \le 0 \\ g_{i,k,l} \ge 0 & x_{i,k,l} = 0 \end{cases} \end{aligned} \tag{12}$$

where $x_{i,k,l}$ is the edge weight corresponding to $g_{i,k,l}$. The piecewise function in equation 12 can be rewritten as

$$\begin{aligned} & \begin{cases} g_{i,k,l} \le d_{i,k}(\bar{a}_l - 1) - \bar{b}_l M \\ g_{i,k,l} \ge d_{i,k}(\bar{a}_l - 1) - \bar{b}_l M & x_{i,k,l} = 1 \\ g_{i,k,l} \le 0 \\ g_{i,k,l} \ge 0 & x_{i,k,l} = 0 \end{cases} \\ \Rightarrow & \begin{aligned} & g_{i,k,l} \le d_{i,k}(\bar{a}_l - 1) - \bar{b} M - M(1 - x_{i,k,l}) \\ & g_{i,k,l} \ge d_{i,k}(\bar{a}_l - 1) - \bar{b} M \\ & g_{i,k,l} \le 0 + M x_{i,k,l} \\ & g_{i,k,l} \ge 0 \end{aligned} \end{aligned} \tag{13}$$

The results of equation 13 obtain a switching effect. When $x_{i,k,l} = 1$, equation 13 becomes

$$\begin{aligned} & g_{i,k,l} \le d_{i,k}(\bar{a}_l - 1) - \bar{b}_l M \\ & g_{i,k,l} \ge d_{i,k}(\bar{a}_l - 1) - \bar{b}_l M \\ & g_{i,k,l} \le M \\ & g_{i,k,l} \ge 0. \end{aligned} \tag{14}$$

The active constraints imply equality for $g_{i,k,l} = (\bar{a}_l - 1) d_{i,k} - \bar{b}_l M$. The inactive constraints imply that $g_{i,k,l}$ is greater then zero, and less then the battery capacity. These constraints are also true, but have no effect on $g_{i,k,l}$. When $x_{i,k,l} = 0$, equation 13 becomes

$$\begin{aligned} & g_{i,k,l} \le d_{i,k}(\bar{a}_l - 1) - \bar{b}_l M - M \\ & g_{i,k,l} \ge d_{i,k}(\bar{a}_l - 1) - \bar{b}_l M \\ & g_{i,k,l} \le 0 \\ & g_{i,k,l} \ge 0. \end{aligned} \tag{15}$$

Where the inactive constraints indicate that $g_{i,k,l}$ is less then some positive value, and greater than a negative value. These constarints have no effect as the active constraints imply equality for $g_{i,k,l} = 0$.

Equation 13 can be expressed in linear form as

$$\begin{aligned} -g_{i,k,l} + d_{i,k}(\bar{a}_l - 1) + x_{i,k,l} &\le M(\bar{b}_l + 1) \\ g_{i,k,l} - d_{i,k}(\bar{a}_l - 1) &\le -\bar{b}_l M \\ g_{i,k,l} - M x_{i,k} &\le 0 \\ -g_{i,k,l} &\le 0. \end{aligned} \tag{16}$$

V. Multi-Graph Additions

An additional contribution this work offers is the expansion to night vs day charging. During the night, there is one charger for each bus; each with a single charge rate. During this time, buses are also available to charge at any time. These differences in operations introduce changes to the original graph formation and warrent a separate graph.

Night graphs consider a situation where both the number of buses reflecte the number of chargers and buses are readily available. Note how there are several source and sink nodes in figure 16. When a bus deploys for the day, the available number of charges changes and are reflected in the underlying source and sink constraints.

Changes in the first graph are reflected in the second through use of state of charge variables.

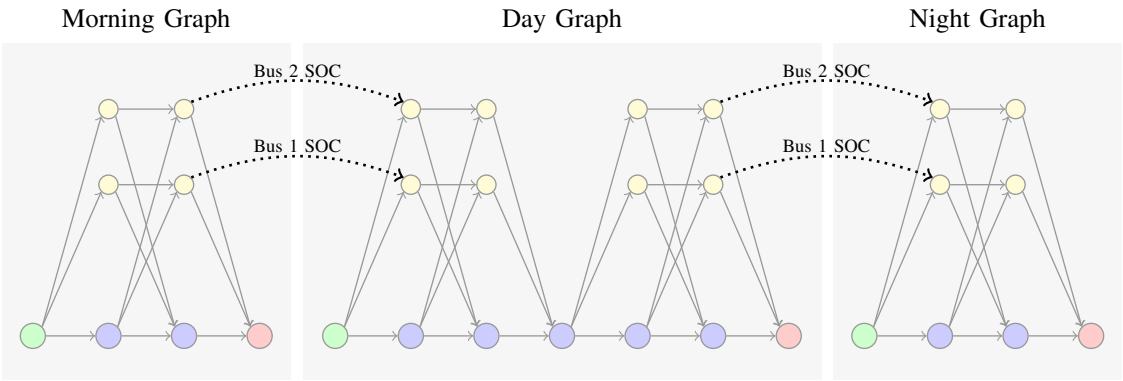

Fig. 16: Night vs Day Graphs

VI. Fiscal Rate Schedule

One objective of this work is to minimize the fiscal cost associated with power use and uses the Rocky Mountain Power schedule 8 billing rates. This billing schedule includes an on-peak power charge, facilities charge, and both on and off peak energy charges.

The facilities charge is computed by calculating the average power over a 15 minute period. The facilities charge is based on the maximum average value over the course of the month. This section of the bill charges $4.81 per kW. The On-Peak Power Charge is similarly calculated but only includes average values from designated on-peak hours. Rocky Mountain Power charges $15.73 per kW for this value.

the facilities power can be formulated as a linear set of constraints that include power used at each timestep for charging buses and external loads. This can be expressed as

$$c_i = \sum_j g_{i,j} + p_i$$

Where c_i represnets the

The energy charges are billed per kWh and charge for each unit of energy used. There are two rates: 5.8282¢for energy consumed during on-peak hours, and 2.6316¢for off-peak hours. general introduction with details for demand and consumption charge and how these relate to the end-of-the-month billing.

a. external loads (contribution) b. consumption charge i. total energy in Kwh ii. on-peak vs off-peak iii. constraints for consumption charge c. demand charge i. average power in 15 minute window ii. on-peak vs facilities iii. constraints for on-peak and facilities charges d. total cost breakdown i. Show how Rocky Mountain Power uses these and what the cost weighting is.

VII. Bus Fleet Operations

Overview of bus operations during the day vs the night a. night environment i. one charger per bus ii. slow chargers iii. single rate chargers iv. buses always available b. day environment i. limited number of chargers ii. fast/variable rates iii. limited charging availability c. multiple graphs to incorporate day vs night charging i. show picture to illustrate this ii. show SOC constraints to implement these relationships

VIII. Objective Function

IX. Gurobi & Usage

X. Results

XI. Future Work

REFERENCES

[1] Avishan Bagherinezhad et al. "Spatio-Temporal Electric Bus Charging Optimization With Transit Network Constraints". In: *IEEE Transactions on Industry Applications* 56.5 (Sept. 2020), pp. 5741–5749. ISSN: 0093-9994, 1939-9367. DOI: 10.1109/TIA.2020.2979132. URL: https://ieeexplore.ieee.org/document/9028116/ (visited on 11/13/2021).

[2] Bhagyashree J Balde and Arghya Sardar. "Electric Road system With Dynamic Wireless charging of Electric buses". In: *2019 IEEE Transportation Electrification Conference (ITEC-India)*. 2019 IEEE Transportation Electrification Conference (ITEC-India). Bengaluru, India: IEEE, Dec. 2019, pp. 1–4. ISBN: 978-1-72813-169-6. DOI: 10.1109/ITEC-India48457.2019.ITECINDIA2019-251. URL: https://ieeexplore.ieee.org/document/9080859/ (visited on 11/18/2021).

[3] T. Boonraksa et al. "Impact of Electric Bus Charging on the Power Distribution System a Case Study IEEE 33 Bus Test System". In: *2019 IEEE PES GTD Grand International Conference and Exposition Asia (GTD Asia)*. 2019 IEEE PES GTD Grand International Conference and Exposition Asia (GTD Asia). Bangkok, Thailand: IEEE, Mar. 2019, pp. 819–823. ISBN: 978-1-5386-7434-5. DOI: 10.1109/GTDAsia.2019.8716023. URL: https://ieeexplore.ieee.org/document/8716023/ (visited on 11/13/2021).

[4] Qifu Cheng et al. "A smart charging algorithm-based fast charging station with energy storage system-free". In: *CSEE Journal of Power and Energy Systems* (2020). ISSN: 20960042, 20960042. DOI: 10.17775/CSEEJPES.2020.00350. URL: https://ieeexplore.ieee.org/stamp/stamp.jsp?tp=&arnumber=9171658 (visited on 11/19/2021).

[5] Blint Csonka. "Optimization of Static and Dynamic Charging Infrastructure for Electric Buses". In: *Energies* 14.12 (June 13, 2021), p. 3516. ISSN: 1996-1073. DOI: 10.3390/en14123516. URL: https://www.mdpi.com/1996-1073/14/12/3516 (visited on 11/13/2021).

[6] Sanchari Deb, Karuna Kalita, and Pinakeshwar Mahanta. "Impact of electric vehicle charging stations on reliability of distribution network". In: *2017 International Conference on Technological Advancements in Power and Energy (TAP Energy)*. 2017 International Conference on Technological Advancements in Power and Energy (TAP Energy). Kollam: IEEE, Dec. 2017, pp. 1–6. ISBN: 978-1-5386-4021-0. DOI: 10.1109/TAPENERGY.2017.8397272. URL: https://ieeexplore.ieee.org/document/8397272/ (visited on 11/16/2021).

[7] Nader A. El-Taweel and Hany E. Z. Farag. "Incorporation of Battery Electric Buses in the Operation of Intercity Bus Services". In: *2019 IEEE Transportation Electrification Conference and Expo (ITEC)*. 2019 IEEE Transportation Electrification Conference and Expo (ITEC). Detroit, MI, USA: IEEE, June 2019, pp. 1–6. ISBN: 978-1-5386-9310-0. DOI: 10.1109/ITEC.2019.8790598. URL: https://ieeexplore.ieee.org/document/8790598/ (visited on 11/19/2021).

[8] Qiang Gao et al. "Charging Load Forecasting of Electric Vehicle Based on Monte Carlo and Deep Learning". In: *2019 IEEE Sustainable Power and Energy Conference (iSPEC)*. 2019 IEEE Sustainable Power and Energy Conference (iSPEC). Beijing, China: IEEE, Nov. 2019, pp. 1309–1314. ISBN: 978-1-72814-930-1. DOI: 10.1109/iSPEC48194.2019.8975364. URL: https://ieeexplore.ieee.org/document/8975364/ (visited on 11/19/2021).

[9] Adnane Houbbadi et al. "Optimal Charging Strategy to Minimize Electricity Cost and Prolong Battery Life of Electric Bus Fleet". In: *2019 IEEE Vehicle Power and Propulsion Conference (VPPC)*. 2019 IEEE Vehicle Power and Propulsion Conference (VPPC). Hanoi, Vietnam: IEEE, Oct. 2019, pp. 1–6. ISBN: 978-1-72811-249-7. DOI: 10.1109/VPPC46532.2019.8952493. URL: https://ieeexplore.ieee.org/document/8952493/ (visited on 11/13/2021).

[10] Amra Jahic, Mina Eskander, and Detlef Schulz. "Preemptive vs. non-preemptive charging schedule for large-scale electric bus depots". In: *2019 IEEE PES Innovative Smart Grid Technologies Europe (ISGT-Europe)*. 2019 IEEE PES Innovative Smart Grid Technologies Europe (ISGT-Europe). Bucharest, Romania: IEEE, Sept. 2019, pp. 1–5. ISBN: 978-1-5386-8218-0. DOI: 10.1109/ISGTEurope.2019.8905633. URL: https://ieeexplore.ieee.org/document/8905633/ (visited on 11/16/2021).

[11] Shubham Jain et al. "Battery Swapping Technology". In: *2020 5th IEEE International Conference on Recent Advances and Innovations in Engineering (ICRAIE)*. 2020 5th IEEE International Conference on Recent Advances and Innovations in Engineering (ICRAIE). Jaipur, India: IEEE, Dec. 1, 2020, pp. 1–4. ISBN: 978-1-72818-867-6. DOI: 10.1109/ICRAIE51050.2020.9358366. URL: https://ieeexplore.ieee.org/document/9358366/ (visited on 11/18/2021).

[12] Seog Y. Jeong et al. "Automatic Current Control by Self-Inductance Variation for Dynamic Wireless EV Charging". In: *2018 IEEE PELS Workshop on Emerging Technologies: Wireless Power Transfer (Wow)*. 2018 IEEE PELS Workshop on Emerging Technologies: Wireless Power Transfer (WoW). Montral, QC, Canada: IEEE, June 2018, pp. 1–5. ISBN: 978-1-5386-2465-4. DOI: 10.1109/WoW.2018.8450926. URL: https://ieeexplore.ieee.org/document/8450926/ (visited on 11/18/2021).

[13] Inaki Ojer et al. "Development of energy management strategies for the sizing of a fast charging station for electric buses". In: *2020 IEEE International Conference on Environment and Electrical Engineering and 2020 IEEE Industrial and Commercial Power Systems Europe (EEEIC / I&CPS Europe)*. 2020 IEEE International Conference on Environment and Electrical Engineering and 2020 IEEE Industrial and Commercial Power Systems Europe (EEEIC / I&CPS Europe). Madrid, Spain:

IEEE, June 2020, pp. 1–6. ISBN: 978-1-72817-455-6. DOI: 10.1109/EEEIC/ICPSEurope49358.2020.9160716. URL: https://ieeexplore.ieee.org/document/9160716/ (visited on 11/16/2021).

[14] Kavuri Poornesh, Kuzhivila Pannickottu Nivya, and K. Sireesha. "A Comparative study on Electric Vehicle and Internal Combustion Engine Vehicles". In: *2020 International Conference on Smart Electronics and Communication (ICOSEC)*. 2020 International Conference on Smart Electronics and Communication (ICOSEC). Trichy, India: IEEE, Sept. 2020, pp. 1179–1183. ISBN: 978-1-72815-461-9. DOI: 10.1109/ICOSEC49089.2020.9215386. URL: https://ieeexplore.ieee.org/document/9215386/ (visited on 11/13/2021).

[15] Nan Qin et al. "Numerical analysis of electric bus fast charging strategies for demand charge reduction". In: *Transportation Research Part A: Policy and Practice* 94 (Dec. 2016), pp. 386–396. ISSN: 09658564. DOI: 10.1016/j.tra.2016.09.014. URL: https://linkinghub.elsevier.com/retrieve/pii/S096585641630444X (visited on 11/13/2021).

[16] Daniel Stahleder et al. "Impact Assessment of High Power Electric Bus Charging on Urban Distribution Grids". In: *IECON 2019 - 45th Annual Conference of the IEEE Industrial Electronics Society*. IECON 2019 - 45th Annual Conference of the IEEE Industrial Electronics Society. Lisbon, Portugal: IEEE, Oct. 2019, pp. 4304–4309. ISBN: 978-1-72814-878-6. DOI: 10.1109/IECON.2019.8927526. URL: https://ieeexplore.ieee.org/document/8927526/ (visited on 11/16/2021).

[17] Ran Wei et al. "Optimizing the spatio-temporal deployment of battery electric bus system". In: *Journal of Transport Geography* 68 (Apr. 2018), pp. 160–168. ISSN: 09666923. DOI: 10.1016/j.jtrangeo.2018.03.013. URL: https://linkinghub.elsevier.com/retrieve/pii/S0966692317306294 (visited on 11/13/2021).

[18] Justin Whitaker et al. "A Network Flow Approach to Battery Electric Bus Scheduling". In: (2021), p. 10.

[19] Xian Zhang and Guibin Wang. "Optimal dispatch of electric vehicle batteries between battery swapping stations and charging stations". In: *2016 IEEE Power and Energy Society General Meeting (PESGM)*. 2016 IEEE Power and Energy Society General Meeting (PESGM). Boston, MA, USA: IEEE, July 2016, pp. 1–5. ISBN: 978-1-5090-4168-8. DOI: 10.1109/PESGM.2016.7741893. URL: http://ieeexplore.ieee.org/document/7741893/ (visited on 11/18/2021).

[20] Dan Zhou et al. "Optimization Method of Fast Charging Buses Charging Strategy for Complex Operating Environment". In: *2018 2nd IEEE Conference on Energy Internet and Energy System Integration (EI2)*. 2018 2nd IEEE Conference on Energy Internet and Energy System Integration (EI2). Beijing: IEEE, Oct. 2018, pp. 1–6. ISBN: 978-1-5386-8549-5. DOI: 10.1109/EI2.2018.8582378. URL: https://ieeexplore.ieee.org/document/8582378/ (visited on 11/13/2021).